The Role of Solation–Contraction Coupling in Regulating Stress Fiber Dynamics in Nonmuscle Cells

John Kolega, Lee W. Janson, and D. Lansing Taylor

Department of Biological Sciences and Center for Fluorescence Research in Biomedical Sciences, Carnegie Mellon University, Pittsburgh, Pennsylvania 15213

Abstract. Serum-deprived Swiss 3T3 fibroblasts constitutively form stress fibers at their edges. These fibers move centripetally towards the perinuclear region where they disassemble. Serum stimulation causes shortening of fibers in a manner suggesting active actin–myosin-based contraction (Giuliano, K. A. and D. L. Taylor. 1990. *Cell Motil. and Cytoskeleton.* 16:14–21). To elucidate the role of actin-based gel structure in these movements, we examined the effects of disrupting actin organization with cytochalasin. Serum-deprived fibroblasts were microinjected with rhodamine analogs of actin or myosin II and fiber dynamics were monitored with a multimode light microscope workstation using video-enhanced contrast and fluorescence modes. When cells were perfused with ≥ 3 μM cytochalasin B or 0.5 μM cytochalasin D, formation and transport of stress fibers were reversibly inhibited, and rapid and immediate shortening of existing fibers was induced. Quantification of actin and myosin II fluorescence associated with individual shortening fibers demonstrated that fluorescence per length of fiber increased for both components, suggesting sliding filament contraction. However, there was also a net loss of both actin and myosin II from fibers as they shortened, indicating a self-destructive process. Loss of material from fibers coupled with increased overlap of actin and myosin II remaining in the fibers suggested that contraction could be induced not only by increasing the force exerted by contractile motors, but also by decreasing gel structure through partial solation. Finally, cytochalasin accelerated contraction of actin–myosin-based gels reconstituted from purified proteins in the absence of myosin-based regulation, further supporting solation–contraction coupling as a possible mechanism for modulating cytoplasmic contractility (Taylor, D. L. and M. Fechheimer. 1982. *Philos. Trans. R. Soc. Lond. B. Biol. Sci.* 299:185–197).

In a simplified model of cell crawling suggested by the behavior of giant amoebae, locomotion is believed to be brought about by the following cycle of events: solated cytoplasm (endoplasm) streams forward to the leading edge, where it is recruited into a cortical gel (ectoplasm). The cortical gel exhibits a rearward transport away from the leading edge, with the leading edge being determined, in part, by a partial decrease in gelation. The rearward transport involves a contraction and results in the exertion of a tractional force on the substratum via linkages across the plasma membrane. Contraction is coupled to solation of the cortical gel, with the solated components being recruited into the forward stream and driven forward under positive hydrostatic pressure to continue the cycle (Taylor and Condeelis, 1979; Taylor and Fechheimer, 1982).

An essential element of this model is the rearward movement of material at or near the cell surface. Such movement has been dubbed "ectoplasmic contraction" by those studying amoebae (for reviews see Taylor and Condeelis, 1979; and Taylor and Fechheimer, 1982) and "cortical flow" by others (Bray and White, 1988). Cortical flow has been observed during movement of a wide range of cell types, including another classic model of cell migration, the translocation of fibroblasts in culture. Recently, Giuliano and Taylor (1990) observed that stress fibers in serum-deprived Swiss 3T3 fibroblasts also undergo constitutive transport from the cell periphery toward the cell center, even in the absence of translocation of the whole cell. Fibers continuously form at the periphery of the cell, move centripetally through the peripheral cytoplasm, and disassemble in the perinuclear region. Furthermore, like the cortical gel of the amoeba model, these fibers are contractile. Extensive contraction of these fibers is triggered by stimulation with growth factors, which also elicits increased locomotive activity in the form of ruffling, the formation of spreading protrusions, and cell translocation (Giuliano and Taylor, 1990). We seek to understand the regulation of this behavior using the simple amoeba model of cell motility as a point of reference.

How cytoplasmic contraction is regulated is not completely understood. Much attention has been paid to the role of myosin II, based on its function in skeletal and smooth muscle. In smooth muscle fibers, contraction can be stimulated by phosphorylation of the regulatory light chain of myosin II and inhibited by antagonists of this phosphorylation

(Seller and Adelstein, 1987; Itoh et al., 1989). In nonmuscle cells, increased light chain phosphorylation occurs during the reorganization of stress fibers induced by growth factor stimulation of quiescent fibroblasts (Bockus and Stiles, 1984), and during contraction of extracted cell models (Masuda et al., 1984). Conversely, Lamb et al. (1988) have reported that dephosphorylation of myosin II regulatory light chain leads to stress fiber breakdown. Furthermore, growth factor stimulation affects many intracellular regulatory pathways other than myosin II phosphorylation, including calcium levels and phosphatidyl inositol metabolism (reviewed by McNeil and Taylor, 1987). These particular pathways, in turn, can affect the state of actin polymerization in the cell, further modifying the contractile machinery.

An additional mechanism for regulating contraction is offered by the solation–contraction coupling hypothesis, which proposes that a cytoplasmic gel can be induced to contract not only by increasing contractile force from a motor, but by decreasing the resistance to that force (reviewed by Taylor and Fechheimer, 1982). As discussed in detail by Taylor and Fechheimer (1982), this model presents these six major postulates: an actin–filament-based gel is a significant structural component of the cytoplasm; in its most rigid state, this gel resists contraction; the gel can be weakened by dissociation of crosslinks between filaments and/or by restriction of filament length; a weakened gel cannot resist contraction, but can transmit forces of contraction through its remaining structure; cytoplasmic contraction can be induced by localized decreases in gel structure; and solation-induced contraction releases smaller pieces of gel and some fraction of the gel's structural and contractile components into the soluble (nongelled) cytoplasm, and as such can be regarded as a "self-destructive" process. Various aspects of the hypothesis have been explored in vitro and in vivo, including the possible role of actin gels in cytoplasmic structure (Luby-Phelps et al., 1988), the role of dissociation of actin crosslinkers in solation (Simon et al., 1988), and the role of solation in initiating contraction (Taylor and Fechheimer, 1982).

In the following study, we use cytochalasin as an agent for solating actin-based gels based on its effect of restricting the length of actin filaments (Hartwig and Stossel, 1979; MacLean-Fletcher and Pollard, 1980). We report that cytochalasin not only inhibits fiber formation and transport in serum-deprived fibroblasts, but also initiates a "self-destructive" contraction as predicted by the solation–contraction coupling hypothesis.

Materials and Methods

Reagents

Tissue culture media and supplements were purchased from Gibco/BRL (Grand Island, NY). Cytochalasin B and cytochalasin D were from Sigma Chemical Co. (St. Louis, MO). Acetamido-tetramethylrhodamine analogs of rabbit skeletal muscle actin (AR-actin) and chicken smooth muscle myosin II (AR-myosin II) were prepared as described by DeBiasio et al. (1988). Calcium-independent myosin light chain kinase was generously provided by Drs. T. Cornwell, J. Sellers, and R. Adelstein (National Institutes of Health, Bethesda, MD).

Cell Culture

Swiss 3T3 murine fibroblasts (no. CCL92) were obtained from American Type Culture Collection (Rockville, MD) and were used between passages 119 and 129. Cells were grown in DME supplemented with 10% calf serum at 37°C in a water-saturated, 5% CO_2, atmosphere. For microscopy, cells were seeded at 500 cells/cm^2 on glass coverslips in DME with 10% calf serum and allowed to attach overnight. Cells were then serum deprived by changing the medium to DME with 0.2% calf serum and incubating an additional 48 h. These serum-deprived fibroblasts are excellent cells in which to analyze fiber dynamics, since the cells do not translocate but their stress fibers exhibit well-defined dynamic behavior (Giuliano and Taylor, 1990; Kolega and Taylor, 1991).

Microinjection

Fluorescent analogs were microinjected as previously described (Amato et al., 1983). AR-myosin II was injected in a buffer consisting of 2 mM Hepes, pH 7.5, 0.2 mM ATP, 1 mM DTT, 0.1 mM EGTA, and 100 mM NaCl. AR-actin was injected in 2 mM Pipes, pH 7.0, 0.1 mM ATP, 0.1 mM DTT, and 0.05 mM $MgCl_2$. After microinjection, cells were rinsed with fresh culture medium and allowed to recover for at least two hours before mounting for observation.

Microscopy

Living cells on glass coverslips were mounted in a closed chamber equipped with ports for perfusion (Focht Chamber; Biological Detection Systems, Inc., Pittsburgh, PA) and maintained at 37°C. This chamber was placed on the stage of a multi-mode light microscope workstation that allows rapid acquisition of images at regular, programmable intervals using both fluorescent and video-enhanced differential-interference contrast optics. The design for this set up is described by Giuliano et al. (1990). Digital images were acquired with a cooled CCD camera (model 200; Photometrics, Tucson, AZ) containing a 512 × 512 pixel frame transfer CCD array (Texas Instruments Inc., Dallas, TX). A parfocal video camera and differential-interference contrast optics were used for focusing the specimen and then fluorescence excitation was used only for the short interval required for fluorescence image acquisition so that photochemical damage was kept to a minimum. Over 60 fluorescence images could be acquired from a single cell with no apparent adverse affects on cell activity or morphology.

Cells that had been microinjected with AR-myosin were photobleached using a multi-line argon laser from Ion Laser Technology (model 5400; Salt Lake City, UT). The beam was directed onto the specimen through the epi-illumination pathway via a half-silvered mirror inserted between the light source and the microscope. To bleach lines on cells, the beam was focused in the image plane in a neighboring field and then the cell was passed through the beam at a constant speed using a motor-driven stage.

Image Analysis

Measurements were made on the digitized video images using an image processor (Perceptics, Knoxville, TN). All images were within the four log units of linearity of the camera used. Fiber fluorescence was always well above the background dark current, and there were no saturated pixels in any of the raw images. Fibers were selected for analysis with the only criteria being that they be visible for at least 20 min of the experiment under examination and that they be distinguishable from surrounding fibers during that interval. To measure the centripetal displacement of a fiber during transport, a line was drawn lying perpendicular to the nearest edge of the cell and passing through the midpoint of the fiber. Fiber displacement was then measured from the point where the fiber intersects this line at each timepoint. Fiber shortening was usually measured from the ends of fibers, but could also be measured from the semi-sarcomeric spacing of myosin II or from discrete reference points that were visible along the lengths of the fibers (Giuliano and Taylor, 1990; Kolega and Taylor, 1991). To quantify the fluorescence intensity of a single fiber, the fiber was traced using an interactive, mouse-driven graphics display. Pixel intensity was then integrated within the outlined region. To correct for photobleaching, fiber intensity was divided by total cell fluorescence (the intensity obtained by integrating over the entire cell) at the same timepoint. The total extent of photobleaching over the longest sequence of images taken was <12%.

For photographic reproduction, images were enhanced by transformation with a linear intensity map, sharpened using a high-pass spatial filter and then photographed from the video monitor.

In Vitro Reconstitution

The techniques for reconstituting actin-based gels and the methods for purification of the constituent proteins are described in detail in the accom-

panying paper (Janson et al., 1991). In the experiments described in the present paper, the gels were made with 1.5 mg/ml rabbit skeletal muscle actin. Filament length was controlled using the calcium-independent, 45-kD fragment of gelsolin, purified from bacteria expressing the clone for this peptide (Way et al., 1989). Average filament length was determined from fluorescence images of phalloidin-labeled samples (Janson et al., 1991) to be 5.5 μm. Polymerized actin was mixed with chicken gizzard filamin and myosin II at ratios of 50/1 actin:filamin and 100/1 actin:myosin II. Final concentration of other components were: 10 mM MOPS (pH 7.2), 0.1 mM DTT, 0.005% NaN_3, 50 mM KCl, 2 mM $MgCl_2$, 70–80 mM NaCl, 200 μM $CaCl_2$, and 1 mM ATP (gel buffer). Before reconstitution, the myosin II was phosphorylated in vitro with calcium-independent myosin light-chain kinase as described by Janson et al. (1991). The actin-filamin-myosin mixture gelled within 1 min after warming, and was overlaid 2 min after warming with cytochalasin in a volume of gel buffer equal to 10% of the reconstituted protein mixture or with gel buffer alone.

Results

Effects of Cytochalasin on Fiber Formation and Transport

We first examined the effects of cytochalasin on the constitutive formation of stress fibers that occurs in the peripheral cytoplasm of serum-deprived Swiss 3T3 fibroblasts (Giuliano and Taylor, 1990). Cells were microinjected with fluorescent analogs of actin or myosin II, which rapidly equilibrated into existing structures (Amato et al., 1983; Amato and Taylor, 1986; DeBiasio et al., 1988). Fiber dynamics were then monitored by time-lapse acquisition of fluorescence and video-enhanced, differential interference-contrast images of cells during various treatments. In control experiments, where cells were perfused with medium alone, we observed continuous formation of stress fibers at the cell periphery. In contrast, when cells were perfused with $\geq$0.3 μM cytochalasin D, there was a complete and reversible inhibition of fiber formation. Within 5 min of perfusion of the drug, fiber formation stopped, and no new fibers were formed as long as cytochalasin was present. When cytochalasin was washed out by perfusing the chamber with fresh medium, new fiber formation at the margin of the cell was clearly apparent within 5–10 min. We observed complete reversal of inhibition in cells in which fiber formation was blocked by 0.5 μM cytochalasin D for as long as 3 h. Perfusion of cytochalasin B produced similar results, with the exception that higher concentrations ($\geq$2 μM) were required. This is consistent with the five- to 20-fold lower potency of cytochalasin B relative to cytochalasin D in its binding to actin filaments in vitro (Cooper, 1987).

Concomitant with its effects on formation of new fibers, cytochalasin blocked transport of existing fibers. When cells were perfused with cytochalasin D at $\geq$0.3 μM or cytochalasin B at $\geq$2 μM, the speed of centripetal transport dropped sharply. The effect was quite striking when viewed in time-lapse sequences. The inhibition of fiber transport by cytochalasin was demonstrated quantitatively by plotting fiber location against time. Fig. 1 shows the displacements of four fibers in a single cell during perfusion and washout of cytochalasin D. In the presence of drug, transport rates were very low, as is evident from the flattened slopes of the four plots during the period after perfusion. In addition, the inhibition was rapidly reversible, as can be seen by the rising slope immediately following washout. Data pooled from similar plots (for three cells from three separate perfusion experiments with a minimum of four fibers tracked in each cell) yielded

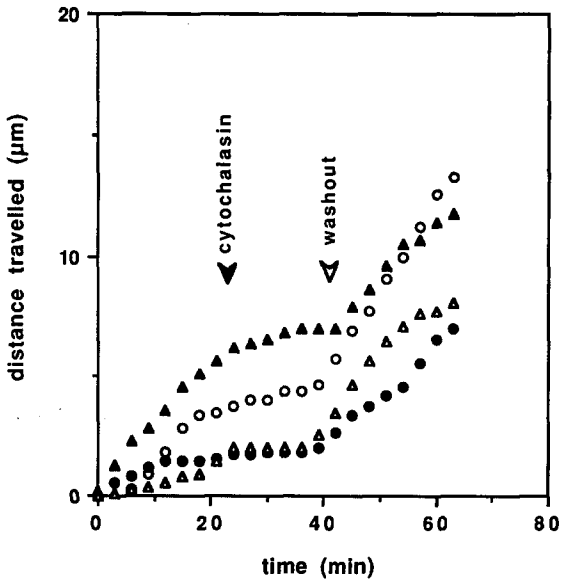

Figure 1. Inhibition of fiber transport by cytochalasin. The movements of four fibers in a typical serum-deprived cell are shown. Distance traveled was measured perpendicular to the nearest cell margin (see Materials and Methods). The four fibers were selected only on the basis that they were "trackable" over a time span >20 min and that they were evenly distributed around the periphery of the cell. At the time indicated by the solid arrow, the cell was perfused with 0.5 μM cytochalasin D, which was subsequently washed out at the time indicated by the hollow arrow. Transport slowed dramatically in the presence of cytochalasin D and increased following washout.

an average rate of fiber transport of 0.14 $\pm$ 0.08 μm/min before treatment. This dropped to 0.04 $\pm$ 0.04 μm/min (71% inhibition) after 5 min in the presence of cytochalasin and rose again to 0.26 $\pm$ 0.09 μm/min (185% recovery) 5 min after washout. The actual degree of inhibition of transport may be even greater because some of the continued centripetal movement in the presence of cytochalasin could be because of contractile events in more proximal cytoplasm (see below). Like the inhibition of fiber formation, the inhibition of transport was rapidly reversible. In fact, immediately after washout the rate of transport was significantly higher than the pretreatment rate. During the time immediately after cytochalasin treatment, there was much less filamentous structure observable in the interfiber cytoplasm. Reduced cytoplasmic structure might offer less hindrance to fiber motion and thereby lead to more rapid transport in this interval (see Luby-Phelps et al., 1988; Simon et al., 1988).

Induction of Fiber Shortening by Cytochalasin

The most striking effect of cytochalasin on serum-deprived cells was the induction of rapid shortening of existing stress fibers (Fig. 2). Within 5 min of perfusion of cytochalasin, most fibers began to shorten. Some fibers shortened from one or both of their ends, i.e., with one end or with the central region remaining stationary. Other fibers fragmented and shortened towards their ends, away from the breakpoint (*arrow* in Fig. 2, t = 3:30). An investigation of the relationship between these fiber ends and substratum adhesions is currently in progress. Fiber length decreased linearly at rates

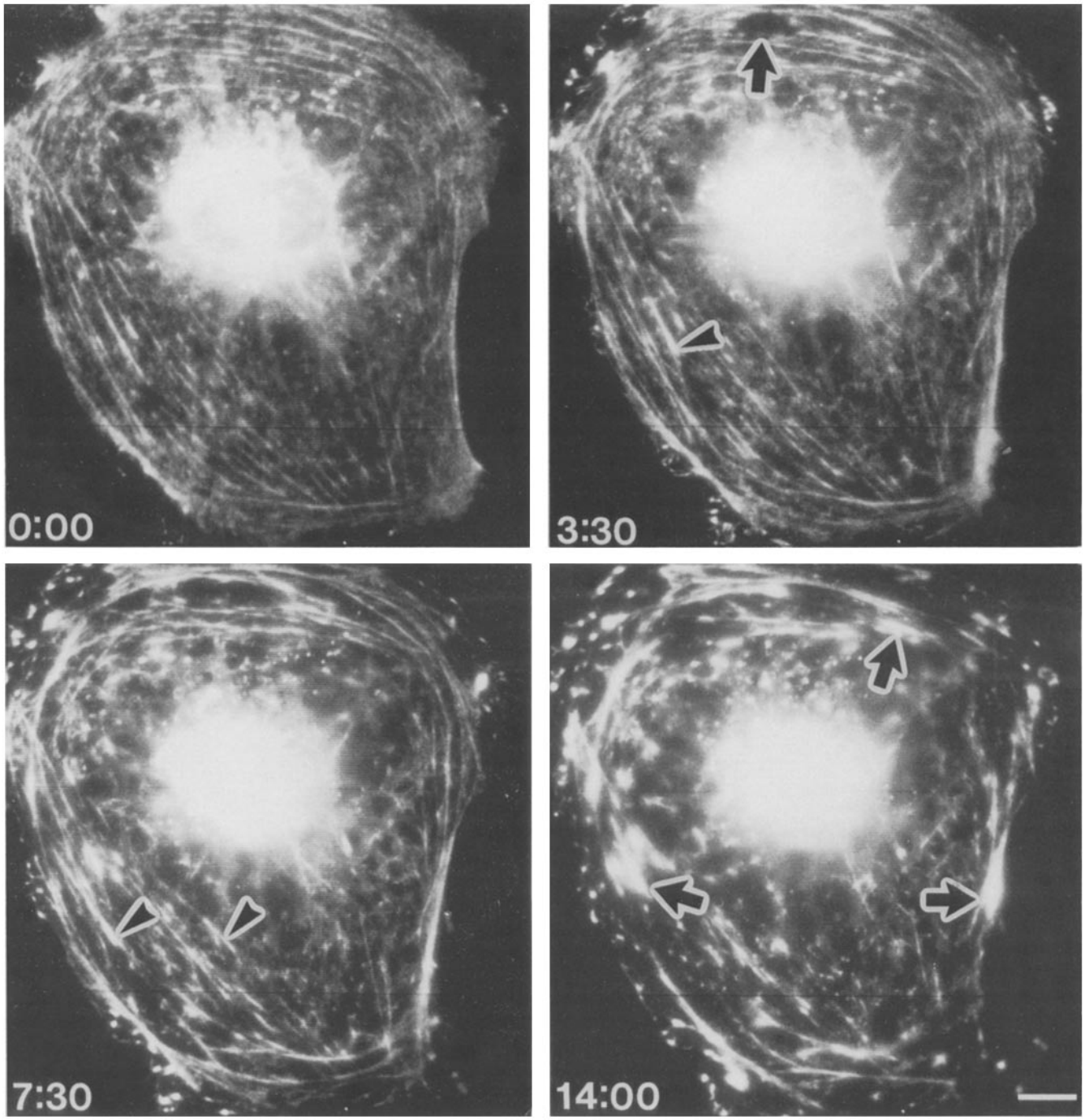

Figure 2. Effects of cytochalasin on serum-deprived cells. Panels show fluorescence images of a single, living, serum-starved Swiss 3T3 fibroblast previously microinjected with AR-myosin II. Time is indicated (min:sec) at the lower left of each image. At t = 0:00, the cell was perfused with 0.5 μM cytochalasin D. An extensive array of stress fibers, most of which lie parallel to the cell's nearest edge, was visible. By t = 3:30, gaps (*arrow*) began to appear in the fiber network as fibers pulled away from each other. A few fibers had already begun to shorten and the density of their associated fluorescence had noticeably increased (*arrowheads*). At t = 7:30, these gaps had become larger and many new gaps had appeared. More stress fibers had shortened and displayed increased concentrations of fluorescence (*arrowheads*). By t = 14:00, most of the stress fibers had shortened into bright foci (*arrows*). Also note that much of the interfiber fluorescence was cleared from large regions of the cytoplasm. Bar, 10 μm.

of 1.6 $\pm$ 0.5 μm/min, until reaching maximal shortening at $\leqslant$20% of the original fiber length (Fig. 3). This compares with a rate of 0.73 $\pm$ 0.39 μm/min observed for fiber shortening in response to serum stimulation (Giuliano and Taylor, 1990; and unpublished data). With prolonged exposure to cytochalasin, a large fraction of the actin- and myosin II–associated fluorescence became concentrated around the nucleus and in a few very bright foci scattered through the more

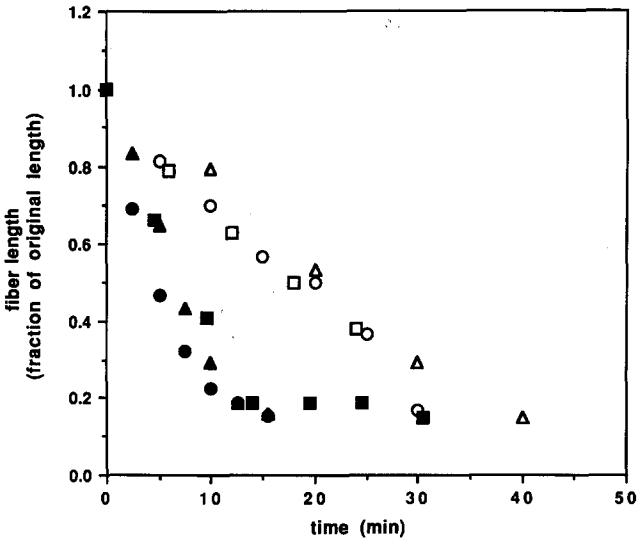

Figure 3. Rate of fiber shortening during cytochalasin treatment. Individual fibers were analyzed during cytochalasin treatment or serum stimulation of serum-deprived cells. Fiber lengths were measured on digitized video images like those shown in Figs. 2 and 5, acquired during the course of treatment. Shown here are time-courses of shortening for three typical fibers for each treatment, with solid symbols representing fibers in cytochalasin-treated cells and open figures indicating fibers in serum-stimulated cells. Different symbol shapes are used for each fiber. In both treatments, shortening persisted at a relatively uniform rate until the fiber had shortened to ~20% of its initial length. However, on average, cytochalasin-induced shortening occurred at twice the rate of serum-stimulated shortening.

peripheral cytoplasm. These foci ultimately became the branchpoints in the highly arborized morphology attained in later stages of cytochalasin treatment.

Video tape replay of the dynamics of fiber shortening very strongly suggested that the fibers contracted. We have demonstrated contraction of stress fibers during serum stimulation by monitoring the decrease in spacing of myosin II (Giuliano and Taylor, 1990). In the present study, cytochalasin treatment caused a rapid loss of the definite sarcomeric structure during shortening, making measurement of individual sarcomeric spacing difficult. However, contraction could be demonstrated by a number of other criteria. To create artificial reference points on shortening fibers, we photobleached two parallel lines across the width of the cell immediately before cytochalasin treatment (Fig. 4, *a* and *b*). The halftime of myosin subunit exchange in fibers is long enough to permit observation of fiber shortening before diffusion obscures the photobleached regions (DeBiasio et al., 1988). Upon perfusion with cytochalasin, these lines moved closer together (Fig. 4, *c* and *d*), indicating a contraction of the intervening cytoplasm. Furthermore, we frequently observed multiple markers on a single fiber, either in the form of photobleached spots (Fig. 5, *arrowheads*) or naturally occurring irregularities in fiber thickness or fluorescence intensity (Fig. 5, *arrows*). Such discrete reference points invariably moved closer together as fibers shortened (Fig. 5). The behavior of endogenous markers was virtually the same whether or not fibers were exposed to laser photobleaching before contraction. We conclude that fibers did not shorten merely by progressive disassembly from their ends.

Further evidence for contraction comes from changes in the density of actin and myosin II along shortening fibers. During shortening, fibers appeared to thicken and condense, their fluorescence images becoming brighter (Fig. 5). This occurred in fibers labeled with the fluorescent analog of either actin or myosin II. We quantified this effect by outlining individual fibers and integrating the fluorescence intensity within each fiber as it shortened. As illustrated in Fig. 6, the fluorescence per length of fiber increased as fibers shortened. This indicates that both actin and myosin II became more concentrated along the fiber, further confirming that fibers contracted and did not shorten solely by depolymerization.

After the onset of contraction, the fluorescence intensities per length were generally slightly lower than predicted for a fiber in which all the actin and myosin is retained in the the shortening fiber (Fig. 6, *solid lines*). This can be explained by a loss of material from within the fiber as it shortens. In a fiber disassembling from its ends, fluorescence per unit length would remain unchanged. As shown in Fig. 7, the total actin and myosin II fluorescence associated with individual fibers decreased by ~50% as they contracted. A number of trivial explanations for this can be discounted. Because fiber fluorescence was normalized to total cellular fluorescence at each time point, this cannot be because of photobleaching. Likewise, there was no underestimation of fluorescence arising from camera saturation, as we analyzed only sequences in which fluorescence remained within the linear range of the camera. Quenching should be negligible owing to the large excess of unlabeled endogenous protein (particularly in the case of the actin analog). Finally, out of plane, extrafibrillar material cannot account for the missing fluorescence. Even if it is assumed that such fluorescence is equal to the fluorescence of full-thickness inter-fibrillar cytoplasm, this would amount to <20% of the fluorescence in the region occupied by an uncontracted fiber. Thus, it is reasonable to conclude that a significant portion of the 50% loss of fluorescence during shortening represents actual loss of material from the fiber. This, in turn, suggests that fiber shortening involves partial disassembly of the fiber as the fiber contracts.

Cytochalasin-induced Contraction In Vitro

If the effect of cytochalasin on stress fibers is because of its ability to solate actin-based gel structures (Hartwig and Stossel, 1979; MacLean-Fletcher and Pollard, 1980; Condeelis and Taylor, 1977), then it should be possible to use cytochalasin to stimulate contraction of actin-based gels containing myosin II in vitro. We wished to test this prediction and to establish a system for studying this process in vitro, where we have greater control over the structural elements and their regulators. Toward this end, we added cytochalasin to gels formed from purified cytoskeletal proteins. Actin–myosin II-filamin gels were formed as described in Materials and Methods and overlaid with cytochalasin in gel buffer or with gel buffer alone. With buffer alone, gels contracted very slowly, taking >90 min to reach full contrac-

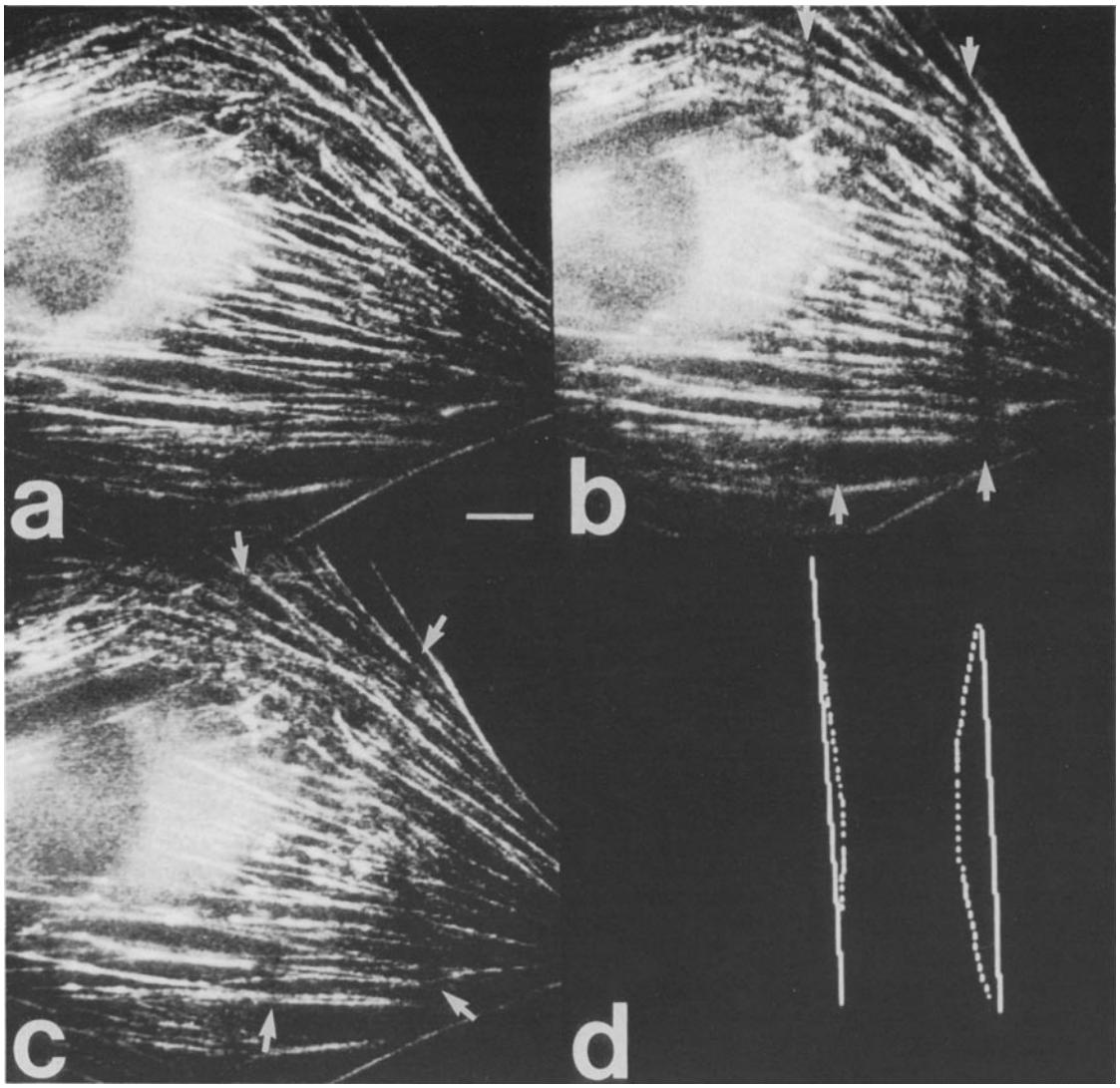

Figure 4. Cytoplasmic contraction during cytochalasin treatment. (*a*) Fluorescence image of a serum-deprived cell microinjected with AR-myosin II. (*b*) Same cell as in *a* after photobleaching two parallel lines (*arrows*). The cell was then perfused with 0.5 μm cytochalasin D. (*c*) 2 min after perfusion. Photobleached lines (*arrows*) were distorted as fibers began to shorten. The lines moved closer together in regions where fibers shortened. (*d*) The center of the photobleached line was traced from *b* (before cytochalasin; *solid line*) and *c* (after cytochalasin; *dotted line*) and superimposed to clearly illustrate their relative displacements. Bar, 10 μm.

tion. But when overlaid with 20 or 50 μM cytochalasin D, contraction was greatly accelerated; the fully contracted state was reached within 15 min (Fig. 8). By comparison, after 60 min, gels overlaid with buffer alone had not contracted beyond the second stage illustrated in Fig. 8.

Discussion

Fiber Formation and Transport

It is not surprising that cytochalasin inhibits the formation of new stress fibers at the periphery of serum-starved cells. Cytochalasin inhibits actin polymerization both in vitro and in vivo (see Cooper, 1987 for review). If filament assembly is blocked, the formation of fibers, larger bundles of filaments, is also necessarily inhibited.

It is less apparent why cytochalasin inhibits transport of existing fibers. One possibility is that continuous polymerization of actin at the cell surface might drive transport of material away from the site of assembly (Wang, 1985). There are several indications that filament assembly occurs at the membrane–cytoplasm interface: actin filaments at the membrane–cytoplasm interface often lie with their barbed ends (the preferred end for monomer addition in vitro) pointed towards the plasma membrane (Small et al., 1978; Mooseker and Tilney, 1975). In living cells microinjected with a fluorescent actin analog, photobleached spots in actin fibers move away from the cell edge toward the cell center (Wang, 1985; DeBiasio, R. L., F. Lanni, and D. L. Taylor, unpublished results), as do filaments visualized by video-enhanced differential-interference contrast microscopy (Fisher et al., 1988), necessitating continuous addition of material at the distal edge. It has also been shown that actin polymerizes preferentially at the distal edge when microinjected into intact cells (Okabe and Hirokawa, 1989).

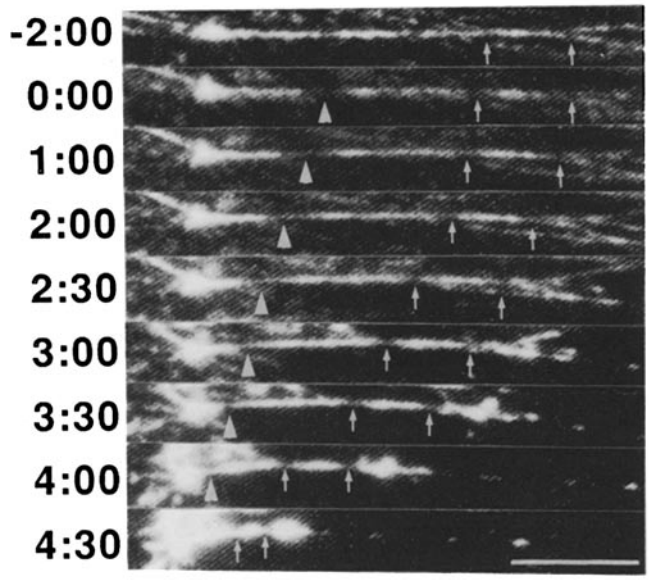

Figure 5. Time-lapse fluorescence images of AR-myosin II in a stress fiber during cytochalasin-induced contraction. Time is indicated (min:sec) to the left of each panel. Immediately after $t = -2:00$, the fiber was marked by photobleaching (dark region indicated by *arrowhead* at $t = 0:00$). At $t = 0:00$, the cell was perfused with 0.5 μM cytochalasin D. Arrowheads follow the centroid of the photobleached spot as the fiber shortened. Straight arrows mark two slightly thinner regions of the fiber that provided additional discrete references. All of these markers drew closer together as the fiber shortened. They also moved closer to the leftmost end of the fiber, which remained almost stationary. Note the increasing thickness and brightness of the fiber during shortening. Bar, 10 μm.

Whether the addition of actin subunits can actually drive the transport of fibers is not known. Forscher and Smith (1988) reported that, while cytochalasin blocks the retrograde streaming of cytoplasm from the peripheral edge in nerve growth cones, more proximal cytoplasm continues to move until the growth cone is "emptied." This suggests that cytochalasin affects only the addition of new material and not the driving force of its transport. However, there is a clear radial orientation of filamentous material in the cells studied by Forscher and Smith (1988). If cytochalasin also induces a contraction, as it does in 3T3 fibroblasts, this could cause radially oriented fibers to draw cytoplasm in towards the cell body, thereby continuing retrograde transport even though distal polymerization has been interrupted.

Alternatively, it may be that neither form of centripetal transport is driven by actin assembly or sliding-filament contraction. The transport observed by Forscher and Smith (1988) involves much smaller structures and occurs at much higher rates (3–6 μm/min) than the movement of stress fibers in serum-deprived fibroblasts (0.1–0.2 μm/min). A motor associated with the membrane–cytoplasm interface could drive both forms of movement, but might move the larger structures less easily. Myosin I, for example, has been shown to bind to plasma membranes and lipid vesicles, and to move organelles along actin filaments in vitro (Pollard et al. 1991). In decreasing actin filament length, whether by capping, severing or increasing nucleation sites (Cooper, 1987; Sampath and Pollard, 1991), cytochalasin may leave only small pieces of filaments for the motor to move, with little or no translocation of larger structures. The distribution of myosin

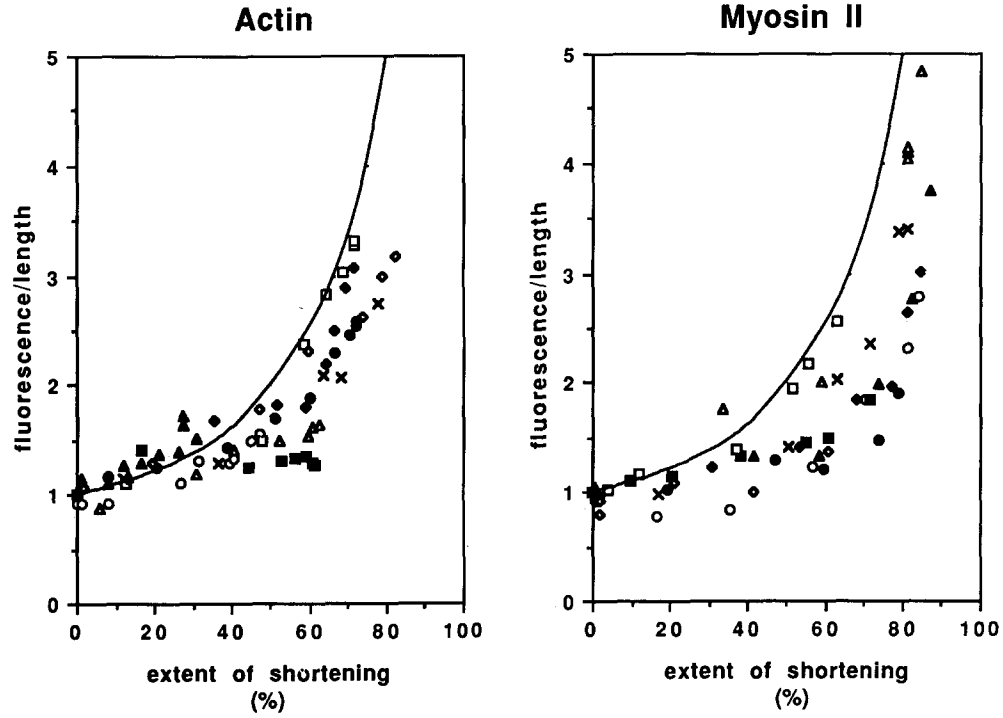

Figure 6. Condensation of actin and myosin during fiber shortening. Individual fibers were tracked during cytochalasin treatment of serum-deprived cells that had previously been injected with AR-actin or AR-myosin II. Shortening is expressed as the percentage of the original fiber length, i.e., at 0%, a fiber has not shortened at all, at the hypothetical maximum of 100% it would have completely disappeared. The average fluorescence intensity per length of fiber was determined as described in Materials and Methods, immediately before treatment and for the same fiber for a minimum of five timepoints during the course of its contraction. Each graph represents data pooled from fibers in three separate experiments. The solid lines indicate the values expected for an ideal fiber contracting without any loss of fluorescence. Note that fluorescence/length for both actin (*left*) and myosin II (*right*) increased as fibers shortened, but was slightly less than the theoretical curve.

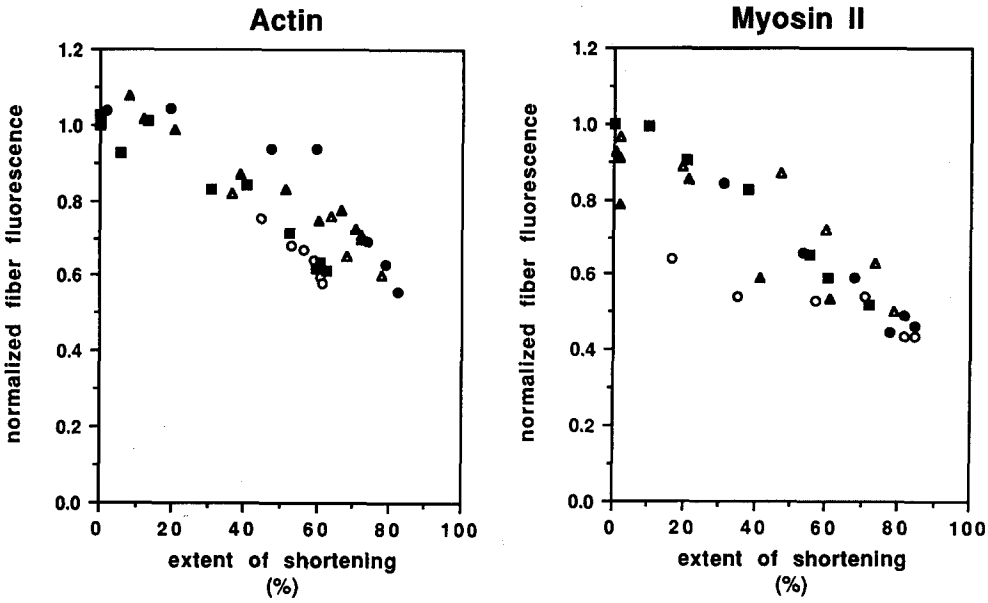

Figure 7. Loss of fiber fluorescence during shortening. Individual fibers were tracked during cytochalasin treatment of serum-deprived cells that had previously been injected with a AR-actin or AR-myosin II. The total fluorescence intensity of each fiber was determined as described in Materials and Methods, immediately before treatment and for the same fiber for a minimum of five timepoints during the course of its shortening. Each graph shows data from five fibers within a single cell, with each symbol representing data from different fibers. All fibers showed a clear decrease in total fluorescence as they shortened. This trend is apparent for fibers labeled with the fluorescent analog of either actin (*left*) or myosin II (*right*).

I in serum-deprived and stimulated cells is described in another study (Conrad et al., manuscript in preparation).

Fiber Shortening

It has long been recognized that cytochalasin causes some form of cytoplasmic contraction (Miranda et al., 1974). In addition, cytochalasin's effects have been shown to require cellular energy metabolism (Miranda et al., 1974; Bershadsky et al., 1980; Schliwa, 1982). Our observations are in full agreement with the view that cytochalasin induces an active contraction and suggests that this is most likely actin–myosin II-based. Both photobleached markers and endoggenous irregularities in stress fibers containing AR-myosin II can be seen to move closer together during fiber shortening, as predicted for a sliding-filament type contraction. Although there is a significant loss of both actin and myosin II fluorescence from shortening fibers, indicating that shortening involves a loss of a fraction of these contractile proteins, we also show that the actin and myosin II that remain become more concentrated as the fibers shorten. This suggests that a sliding-filament contraction occurs coupled to the dispersal (solation) of the fiber. It should be noted that we documented contractility only in relatively large stress fibers, which are easily followed and readily delineated from surrounding structures. A similar process probably occurs with much smaller filamentous elements throughout much of the cytoplasm, as is suggested by the clearing of myosin from the interfibrillar space in our study (Figs. 2 and 5) and the loss of filamentous structure from vast regions of the cytoplasm observed in electron microscopic examinations (Schliwa, 1982).

Stress fiber contraction is most likely a direct effect of

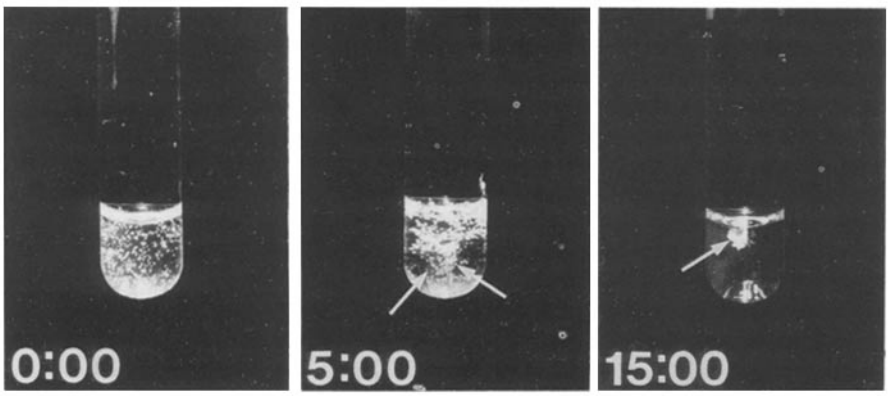

Figure 8. Cytochalasin-induced contraction of gels in vitro. An actin–myosin II-filamin gel was formed as described in Materials and Methods. Two minutes after mixing the components, the gel was overlaid with 20 μM cytochalasin D. Time (min:sec) at lower left of each panel is the time after overlaying cytochalasin. At t = 0:00, a slightly translucent gel could be seen to fill the volume of the tube. At t = 5:00 the gel had begun to contract, pulling away from the walls of the tube. Arrows point to the edges of the retracting gel. By t = 15:00, the gel had contracted completely into a small opaque nodule (*arrow*). Control gels formed simultaneously but overlaid with buffer alone contracted very slowly, and had only reached a stage resembling the center panel at t = 60 min.

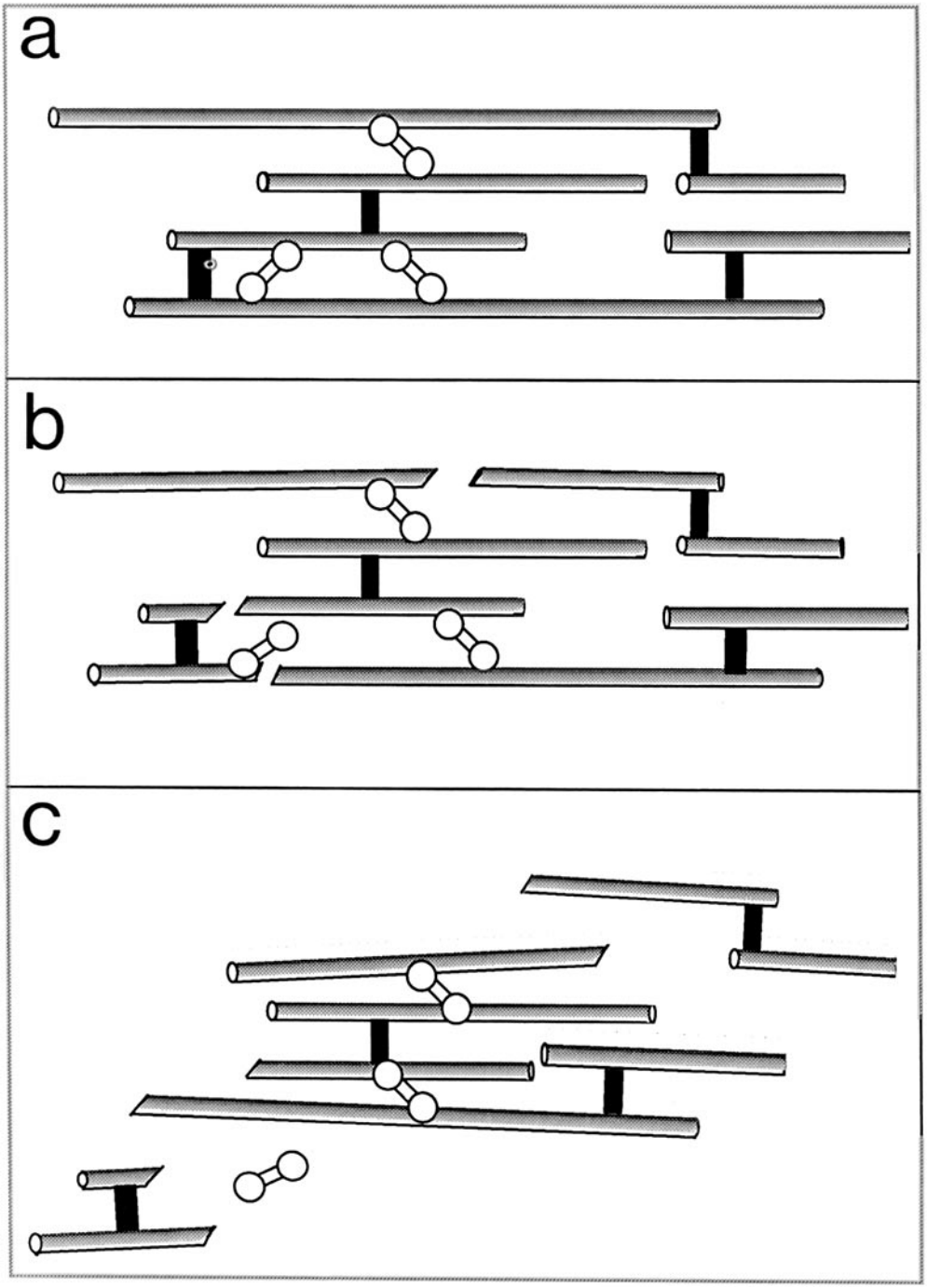

Figure 9. Solation-contraction coupling. This model illustrates three stages of a solation-induced contraction. (*a*) An actin-based gel is represented by actin filaments (*shaded cylinders*) cross-linked by actin-binding proteins (*black bars*) in the presence of a contractile motor (*dumbbells*). If the contractile force is weak or the gel structure very strong, the gel cannot contract. (*b*) It can be caused to contract by increasing the contractile force or by decreasing the gel structure. The latter might occur by disrupting cross-links or by breaking filaments, as depicted here. (*c*) When the gel structure is weakened, the existing contractile motors can, by classic sliding filament motility, cause the gel to contract. Furthermore, the contraction is a "self-destruct" process, as disconnected components are released into the less-structured cytoplasm.

cytochalasin's action on actin filaments, and not a result of some secondary effect on cellular metabolism. First of all, the action of cytochalasin D, which lacks the effects on hexose metabolism associated with cytochalasin B (Rampal et al., 1980), differs from that of cytochalasin B only in the dose required. This difference in potency is proportional to the relative potencies of cytochalasin B and D in blocking actin filament polymerization in vitro (Cooper, 1987). Moreover, both drugs induce stress fiber contraction in cells at approximately the same concentration at which they cap actin filaments in vitro (Cooper, 1987). It is well known that actin subunits exchange rapidly, even in stress fibers, suggesting the dynamic appearance of filament ends (Amato and Taylor, 1986; Luby-Phelps et al., 1984). Finally, contraction can be modulated in actin–myosin II-filamin gels reconstituted from purified cytoskeletal proteins, i.e., in the complete absence of any additional regulatory pathways.

How does cytochalasin cause contraction? Cytochalasin's mechanism is extremely complex (Sampath and Pollard, 1991), but its net effect on actin is a reduction in filament length, an event ultimately leading to solation of gelled networks (see Janson et al., 1991; and references therein). Cytoplasmic extracts from amoeboid cells contract upon treatment with cytochalasin and other conditions that decrease gel structure (Stossel and Hartwig, 1976; Pollard, 1976; Condeelis and Taylor, 1977). This led to the hypothesis that

contraction can result not only from increased motor activity, but also from partial solation of the network and the concomitant reduction in resistance to contraction (Fig. 9; see also Taylor and Fechheimer, 1982). Stossel and colleagues have also proposed an interdependence of contractility and state of gelation (Stendahl and Stossel, 1980; Stossel, 1982). Their model involves only a disconnection of the network elements resisting contraction, whereas we suggest a two-part process wherein partial solation decreases resistance to contraction and also releases gel components into the solated phase in a "self-destruct" manner (Taylor and Fechheimer, 1982).

The smooth muscle paradigm of cellular contractility has focused on regulation of myosin II as the primary means of controlling contraction. Cytochalasin's ability to induce stress fiber contraction suggests that solation of the actin-based gel can also regulate, or at least modulate, contraction in the living cell. Kenney et al. (1990) have found that maximal force generation by smooth muscle myosin is achieved with only 20% of the regulatory light chain phosphorylated. Thus, very low levels of phosphorylation may be sufficient for exerting contractile force in the cell and modulation of the gel structure may be used as an additional regulatory process. Such modulation can be provided by the numerous endogenous proteins known to cap and/or sever actin filaments (e.g., gelsolin, severin, fragmin, actin-depolymerizing factor) and/or by dissociating actin-crosslinking proteins. Several of these actin-binding proteins are regulated by calcium, which has been implicated as a signal in many locomotive events, including the response of quiescent cells to growth-factor stimulation (McNeil and Taylor, 1987). In addition, it has been reported that the phosphatidyl inositol phosphates, which constitute another important set of messengers in the growth-factor stimulation response, can regulate the actin-capping activity of gelsolin (Janmey et al., 1987) and of the calcium-independent actin-capping protein, gCap39 (Yu et al., 1990). Other levels of regulation could also be involved, including such molecules as caldesmon.

Thus, there are many avenues by which a cell could regulate the structure of its actin-based gel and thereby control contraction. To understand what role this might play in cell motility, we must determine how the cell balances the antagonistic forces of contractility and rigidity of the gel structure. How are these forces coordinated on a local basis within the cell during shape changes and locomotion? How is the polarity of the gelation-solation cycle maintained? How many regulatory or modulatory mechanisms exist beyond myosin II phosphorylation and solation–contraction coupling? We believe that many answers lie in the two-pronged attack of probing the living cell with specific effectors of cytoplasmic structure and contractility, and characterizing the actions of these agents in the precisely controlled environment of in vitro reconstitutions. The latter approach is used in the paper that follows (Janson et al., 1991), wherein we analyze the effects of filament length, crosslinking, and contractile force on the morphology and contractility of actin–myosin II gels.

We thank J. Montibeller, for generating seemingly limitless supplies of myosin and its fluorescent analogs, and Drs. K. Giuliano and F. Lanni, for many helpful discussions and for critically reading the manuscript.

This research was supported by grants AR-32461, GM-34639, and 5T32GM08067-08 from the National Institutes of Health, and DIR-8907855 from the National Science Foundation.

Received for publication 15 February 1991 and in revised form 24 May 1991.

References

Amato, P. A., and D. L. Taylor. 1986. Probing the mechanism of incorporation of fluorescently labeled actin into stress fibers. *J. Cell Biol.* 102:1074–1084.

Amato, P. A., E. R. Unanue, and D. L. Taylor. 1983. Distribution of actin in spreading macrophages: a comparative study on living and fixed cells. *J. Cell Biol.* 96:750–761.

Bershadsky, A. D., V. I. Gelfand, T. M. Svitkina, and I. S. Tint. 1980. Destruction of microfilament bundles in mouse embryo fibroblasts treated with inhibitors of energy metabolism. *Exp. Cell Res.* 127:421–429.

Bockus, B. J., and C. D. Stiles. 1984. Regulation of cytoskeletal architecture by platelet-derived growth factor, insulin and epidermal growth factor. *Exp. Cell Res.* 153:186–197.

Bray, D., and J. G. White. 1988. Cortical flow in animal cells. *Science (Wash. DC).* 239:883–888.

Condeelis, J. S., and D. L. Taylor. 1977. The contractile basis of amoeboid movement V. The control of gelation, solation and contraction in extracts of *Dictyostelium discoideum*. *J. Cell Biol.* 74:901–927.

Cooper, J. A. 1987. Effects of cytochalasin and phalloidin on actin. *J. Cell Biol.* 105:1473–1478.

DeBiasio, R. L., L.-L. Wang, G. W. Fisher, and D. L. Taylor. 1988. The dynamic distribution of fluorescent analogs of actin and myosin in protrusions at the leading edge of migrating Swiss 3T3 fibroblasts. *J. Cell Biol.* 107:2631–2645.

Fisher, G. W., P. A. Conrad, R. L. DeBiasio, and D. L. Taylor. 1988. Centripetal transport of cytoplasm, actin, and the cell surface in lamellipodia of fibroblasts. *Cell Motil. and Cytoskeleton.* 11:235–247.

Forscher, P., and S. J. Smith. 1988. Actions of cytochalasins on the organization of actin filaments and microtubules in a neuronal growth cone. *J. Cell Biol.* 107:1505–1516.

Giuliano, K. A., and D. L. Taylor. 1990. Formation, transport, contraction and disassembly of stress fibers in fibroblasts. *Cell Motil. and Cytoskeleton.* 16:14–21.

Giuliano, K. A., M. A. Nederlof, R. DeBiasio, F. Lanni, A. S. Waggoner, and D. L. Taylor. 1990. Multi-mode light microscopy. *In* Optical Microscopy for Biology. B. Herman and K. Jacobson, editors. Wiley-Liss, New York. 543–557.

Hartwig, J. H., and T. P. Stossel. 1979. Cytochalasin B and the structure of actin gels. *J. Mol. Biol.* 134:539–553.

Itoh, T., M. Ikebe, G. J. Kargacin, D. J. Hartshorne, B. E. Kemp, and F. S. Fay. 1989. Effects of modulators of myosin light-chain kinase activity in single smooth muscle cells. *Nature (Lond.).* 338:164–167.

Janmey, P. A., K. Ida, H. L. Yin, and T. P. Stossel. 1987. Polyphosphoinositide micelles and polyphosphoinositide-containing vesicles dissociate endogenous actin-gelsolin complexes and promote actin assembly from the fast-growing ends of actin filaments blocked by gelsolin. *J. Biol. Chem.* 262: 12228–12236.

Janson, L. W., J. Kolega, and D. L. Taylor. 1991. Modulation of contraction by gelation/solation in a reconstituted motile model. *J. Cell Biol.* 114: 1005–1015.

Kenney, R. E., P. E. Hoar, and W. G. L. Kerrick. 1990. The relationship between ATPase activity, isometric force and myosin light-chain phosphorylation. *J. Biol. Chem.* 265:8642–8649.

Kolega, J., and D. L. Taylor. 1991. Regulation of actin and myosin-II dynamics in living cells. *In* Ordering the Membrane-Cytoskeleton Trilayer. J. S. Morrow and M. S. Mooseker, editors. Academic Press, New York. In press.

Lamb, N. J. C., A. Fernandez, M. A. Conti, R. Adelstein, D. B. Glass, W. J. Welch, and J. R. Feramisco. 1988. Regulation of actin microfilament integrity in living nonmuscle cells by the cAMP-dependent protein kinase and the myosin light chain kinase. *J. Cell Biol.* 106:1955–1971.

Luby-Phelps, K., P. A. Amato, and D. L. Taylor. 1984. Selective immunocytochemical detection of fluorescent analogs with antibodies specific for the fluorophore. *Cell Motil. and Cytoskeleton.* 4:137–150.

Luby-Phelps, K., F. Lanni, and D. L. Taylor. 1988. The submicroscopic properties of cytoplasm as a determinant of cellular function. *Annu. Rev. Biophys. Biophys. Chem.* 17:369–396.

MacLean-Fletcher, S., and T. P. Pollard. 1980. Mechanism of action of cytochalasin B on actin. *Cell.* 20:329–341.

Masuda, H., K. Owaribe, H. Hayashi, and S. Hatano. 1984. Ca^{2+}-dependent contraction of human lung fibroblasts treated with TX-100: a role of Ca^{2+}-calmodulin-dependent phosphorylation of myosin 20,000-Dalton light chain. *Cell Motil. and Cytoskeleton.* 4:315–331.

McNeil, P. L., and D. L. Taylor. 1987. Early cytoplasmic signals and cytoskeletal responses initiated by growth factors in cultured cells. *In* Cell Membranes, Vol. 3. E. Elson, W. Frazier, and L. Glaser, editors. Plenum Publishing Corp. New York. 365–405.

Miranda, A. F., G. C. Godman, A. D. Deitch, and S. W. Tanenbaum. 1974.

Action of cytochalasin D on cells of established lines. I. Early events. *J. Cell Biol.* 61:481–500.

Mooseker, M. S., and L. G. Tilney. 1975. The organization of an actin filament-membrane complex: filament polarity and membrane attachment in the microvilli of intestinal epithelial cells. *J. Cell Biol.* 67:725–743.

Okabe, S., and N. Hirokawa. 1989. Incorporation and turnover of biotin-labeled actin microinjected into fibroblastic cells: an immunoelectron microscopic study. *J. Cell Biol.* 109:1581–1595.

Pollard, T. P. 1976. The role of actin in temperature-dependent gelation and contraction of extracts of *Acanthamoeba*. *J. Cell Biol.* 68:579–601.

Pollard, T. P., S. K. Doberstein, and H. G. Zot. 1991. Myosin-I. *Annu. Rev. Physiol.* 53:653–681.

Rampal, A. L., H. B. Pinokofsky, and C. Y. Jung. 1980. Structure of cytochalasins and cytochalasin B binding site in human erythrocyte membranes. *Biochemistry.* 19:679–683.

Sampath, P., and T. D. Pollard. 1991. Effects of cytochalasin, phalloidin, and pH on the elongation of actin filaments. *Biochemistry.* 30:1973–1980.

Schliwa, M. 1982. Action of cytochalasin D on cytoskeletal networks. *J. Cell Biol.* 92:79–91.

Sellers, J. R., and R. S. Adelstein. 1987. Regulation of contractile activity. *In* The Enzymes, Vol. 18. P. D. Boyer and E. G. Krebs, editors. Academic Press, Inc., Orlando, FL. 381–418.

Simon, J. R., R. H. Furukawa, B. R. Ware, and D. L. Taylor. 1988. The molecular mobility of alpha-actinin and actin in a reconstituted model of gelation. *Cell Motil. and Cytoskeleton.* 11:64–82.

Small, J. V., G. Isenberg, and J. E. Celis. 1978. Polarity of actin at the leading edge of cultured cells. *Nature (Lond.).* 272:638–639.

Stendahl, O. I., and T. P. Stossell. 1980. Actin-binding protein amplifies contraction, and gelsolin confers calcium control on the direction of contraction. *Biochem. Biophys. Res. Comm.* 92:675–681.

Stossel, T. P. 1982. The structure of cortical cytoplasm. *Philos. Trans. R. Soc. Lond. B. Biol. Sci.* 299:275–289.

Stossel, T. P., and J. H. Hartwig. 1976. Interaction of actin, myosin, and a new actin-binding protein of rabbit pulmonary macrophages. II. Role in cytoplasmic movement and phagocytosis. *J. Cell Biol.* 68:602–619.

Taylor, D. L., and J. S. Condeelis. 1979. Cytoplasmic structure and contractility in amoeboid cells. *Int. Rev. Cytol.* 56:57–143.

Taylor, D. L., and M. Fechheimer. 1982. Cytoplasmic structure and contractility: the solation-contraction hypothesis. *Phil. Trans. R. Soc. Lond. B. Biol. Sci.* 299:185–197.

Wang, Y.-L. 1985. Exchange of actin subunits at the leading edge of living fibroblasts: possible role of treadmilling. *J. Cell Biol.* 101:597–602.

Way, M., J. Gooch, B. Pope, and A. G. Weeds. 1989. Expression of human plasma gelsolin in *Escherichia coli* and dissection of actin binding sites by segmental deletion mutagenesis. *J. Cell Biol.* 109:593–605.

Yu, F.-X., P. A. Johnston, T. C. Sudhof, and H. L. Yin. 1990. gCap39, a calcium ion- and polyphosphoinositide-regulated actin capping protein. *Science (Wash. DC).* 250:1413–1415.